Article

Journal of
Nanoscience and Nanotechnology
Vol. 16, 9843–9850, 2016
www.aspbs.com/jnn

Magnetic Co(II) Porphyrin Nanospheres Appending Different Substituent Groups Showing Higher Catalytic Activities in Cyclohexane

Ping Zhao[1,*], Min-Chao Liu[1], Min Zheng[2], Shu-Fang Jin[1], Ding-Tong Tang[1],
Jia-Qi Lin[1], Yan-Na Ma[1], Jiong Chen[1], and Hong-Jian Liu[1]

[1] *School of Chemistry and Chemical Engineering, Guangdong Pharmaceutical University,*
Zhongshan 528458, P. R. China
[2] *School of Basic Courses, Guangdong Pharmaceutical University, Education Mega Centre,*
Guangzhou 510006, P. R. China

Magnetic polymer nanospheres immobilizing Co(II) porphyrins with different substituents were prepared and exhibited satisfying size, morphology and magnetic responsiveness. These core/shell structured nanospheres showed much higher catalytic activities in hydroxylating cyclohexane than the non-supported Co(II) porphyrin analogues. Moreover, these magnetic nanospheres could be easily recovered and reused for up to five times with maintaining their high catalytic efficiencies, and thus are good candidates for high-efficient, environmental-friendly catalysts.

Keywords: Nanostructures, Chemical Synthesis, Electron Microscopy, Magnetic Properties.

1. INTRODUCTION

Interests in the field of synthetic metalloporphyrins to mimic cytochrome P-450 monooxygenase (P-450) have mushroomed since the pioneering work of Groves et al. in 1979.[1] The design, synthesis, structure, and catalytic activity research of new catalysts as the analogues of the active sites in metalloenzymes constitute a new research area currently named "biomimetic catalysis." In special, studies involving catalytic oxidation mediated by metalloporphyrins have been increased in many areas such as in the conversion of both saturated and unsaturated hydrocarbons to valuable fine chemicals and oxidation of drugs and pollutants.[2–4]

Previous studies concluded that the catalysis in homogeneous systems is limited by the following drawbacks: the porphyrin ring is liable to oxidative self-destruction and the metalloporphyrins are subject to aggregation through π–π interaction.[3,5] Immobilization of metalloporphyrins on solid supports can offer several advantages over traditional solution-phase chemistry, such as higher stability, increased selectivity, being easily recovered and reused, etc. Among the supports that can be used to immobilize metalloporphyrins, polystyrene derivatives are often employed for their cheapness, ready availability, mechanical robustness, chemical inertness and facile functionalization. Moreover, they can also provide suitable microenvironment for the "accommodation" of porphyrin catalytic centers.[5–10] However, as for polystyrene supported catalysts, troublesome centrifugation or filtration is needed to recycle them, which often causes decreases in catalytic efficiency for the reused catalysts.[12,13] In overcoming such problems, magnetic polymer microspheres arouse our attention due to their specific surface properties, and relatively rapid and effortless magnetic separation.[14–18] In this field, nanometer-sized catalyst supports have recently attracted a great deal of interest because of their high specific surface area and outstanding stability as well as activity in the liquid phase.[19–24] The combination of the easy separation of magnetic polymer microspheres and the special properties of nanometer-sized catalyst supports provides a good opportunity to design and synthesize novel polystyrene supported metalloporphyrins to mimic the function of P450 enzymes.

---

[*] Author to whom correspondence should be addressed.

1533-4880/2016/16/9843/008 doi:10.1166/jnn.2016.12615

Meanwhile, comparative studies of catalytic efficiency in the biomimetic oxidations of hydrocarbons using metalloporphyrins as catalysts take us to conclude that the efficiency is significantly affected by the factors such as steric, metal centre and substituents on porphyrin ring structures.[5–8] However, so far research on the influential factors has been mostly focused on the symmetric catalysis while that on the asymmetric catalysis is relatively rare.

In this paper, a series of magnetic polymer nanospheres immobilizing Co(II) porphyrins appending *p*-OCH_3, *p*-H and *p*-Cl phenyl substituents (designated as MPNSs(CoMP), MPNSs(CoPP) and MPNSs(CoCP), respectively) were synthesized and characterized. The magnetic polymer nanospheres are of core/shell structure in which the core is composed of numerous Fe_3O_4 particles and the shell is composed of a copolymer of styrene and Co(II) porphyrin acrylates. The catalytic performance of these nanospheres for cyclohexane hydroxylation with molecular oxygen was compared with that of non-supported Co(II) porphyrin acrylates. The effects of peripheral subtituents to the catalytic efficiency using different oxidants were also discussed.

2. EXPERIMENTAL DETAILS

2.1. Materials

The precursors, 5-(4-hydroxyl)phenyl-10,15,20-trimethoxyphenylporphyrin (HPTMPP), 5-(4-hydroxyl) phenyl-10,15,20-triphenylporphyrin (HPTPP) and 5-(4-hydroxyl) phenyl-10,15,20-trichlorophenylporphyrin (HPTCPP) were synthesized according to the literature [10]. All other reagents were commercially available.

2.2. Physical Measurements

Elemental analysis (C, H and N) was carried out on a Perkin-Elmer 240 Q elemental analyzer. ESI-MS was measured on a Thermo Finnigan LCQ DECA XP spectrometer. ^{1}H NMR spectra were recorded on a Varian INOVA500NB superconducting Fourier transform nuclear magnetic resonance spectrometry with $CDCl_3$ as solvent at room temperature and TMS as internal standard. UV-Vis and IR spectra were recorded on a Shimadzu UV-3150 spectrophotometer and an Equinox 55 Fourier transformation infra-red spectrometer. The scanning electron microscopy (SEM) analyses were performed with a JSM-6330F field emission scanning electron microscope. The transmission electron microscope (TEM) analyses were performed with a JEM-2010HR transmission electron microscope. The particle sizes were measured by a Mastersizer 2000 laser particle size analyzer. An Iris (HR) inductively coupled plasma (ICP) -atomic emission spectrometer was used to determine the contents of Co(II) porphyrin acrylates and Fe_3O_4. Magnetic measurements were performed by using a XL-7 magnetic property measurement system. The catalytic products were detected by Gas Chromatography (GC-7890II) of Tianmei Co. Ltd.

2.3. Synthesis of Porphyrin Acrylates

Porphyrin acrylates including 5-(4-acryloxy)phenyl-10,15,20-trimethoxyphenylporphyrin (APTMPP), 5-(4-acryloxy)phenyl-10,15,20-triphenylporphyrin (APTPP) and 5-(4-acryloxy)phenyl-10,15,20-trichlorophenylporphyrin (APTCPP) were similarly synthesized. A typical reaction was conducted as follows. A mixture of 50 mL $CHCl_3$ and 0.2500 g HPTMPP was stirred at 60 °C. 2.0 g acrylyl chloride dissolved in 5 mL $CHCl_3$ was added dropwise. After 2 h, the mixture was washed with 5% K_2CO_3 several times and then evaporated to dryness. The crude material was purified on a silica gel chromatograph using $CHCl_3$ and petroleum ether as eluent. APTMPP was obtained as a purple powder. Yield: 0.2128 g (79.2 wt%). ESI-MS [$CHCl_3$, m/z]: 775 ([APTMPP]$^+$). ^{1}H NMR ($CDCl_3$, 500 MHz): δ 8.86 (*m*, 8H, pyrrole ring), 8.20–8.22 (*d*, $J = 8.5$ Hz, 2H), 8.08–8.10 (*d*, $J = 8.6$ Hz, 6H), 7.51–7.52 (*d*, $J = 8.5$ Hz, 2H), 7.22–7.24 (*d*, $J = 8.6$ Hz, 6H), 6.74–6.78 (*m*, 1H), 6.45–6.51 (*m*, 1H), 6.10–6.12 (*m*, 1H), 4.03 (*s*, 9H), −2.73 (*s*, 2H, Pyrrole N–H).

APTPP was similarly prepared by replacing HPTMPP by HPTPP. Yield: 76.5 wt%. ESI-MS [$CHCl_3$, m/z]: 684 ([APTPP]$^+$). ^{1}H NMR($CDCl_3$, 500 MHz): δ 8.84–8.88 (*m*, 8H, pyrrole ring), 8.24–8.26 (*d*, $J = 8.5$ Hz, 2H), 8.20–8.22 (*d*, $J = 8.3$ Hz, 6H), 7.75 (*m*, 6H), 7.73 (*m*, 3H, *p*), 7.53–7.54 (*d*, $J = 8.5$ Hz, 2H), 6.75–6.78 (*m*, 1H), 6.46–6.52 (*m*, 1H), 6.11–6.13 (*m*, 1H), −2.76 (*s*, 2H, Pyrrole N–H).

APTCPP was also similarly prepared by replacing HPTMPP by HPTCPP. Yield: 74.3 wt%. ESI-MS [$CHCl_3$, m/z]: 788 ([APTCPP]$^+$). ^{1}H NMR($CDCl_3$, 500 MHz): δ 8.81–8.88 (*m*, 8H, pyrrole ring), 8.18–8.20 (*d*, $J = 8.6$ Hz, 2H), 8.09–8.10 (*d*, $J = 8.5$ Hz, 6H), 7.69–7.71 (*d*, $J = 8.0$ Hz, 6H), 7.52–7.53 (*d*, $J = 8.6$ Hz, 2H), 6.75–6.79 (*m*, 1H), 6.46–6.52 (*m*, 1H), 6.12–6.14 (*m*, 1H), −2.84 (*s*, 2H, Pyrrole N–H).

2.4. Synthesis of Metalloporphyrin Acrylates

Co(II) porphyrin acrylates including 5-(4-acryloxy)phenyl-10,15,20-trimethoxyphenylporphyrin Co(II) (CoAPTMPP), 5-(4-acryloxy)phenyl-10,15,20-triphenylporphyrin Co(II) (CoAPTPP) and 5-(4-acryloxy)phenyl-10,15,20-trichlorophenylporphyrin Co(II) (CoAPTCPP) were synthesized by a reaction of $Co(Ac)_2$ with corresponding porphyrin acrylates. A typical reaction was conducted as follows. 0.5 g $Co(Ac)_2$ and 1 g NaCl dissolved in 40 mL HAc were mixed with 20 mL $CHCl_3$ solution of APTMPP (0.3180 g). The mixture was stirred at 65 °C for 8 h. Then, the reaction mixture was washed with H_2O and 1 M HCl several times. After washing to neutrality with H_2O, drying over anhydrous Na_2SO_4 and concentrating via rotary evaporation, the residue was chromatographed on a silica gel coluCo using $CHCl_3$ as eluent. Evaporation of solvent afforded CoAPTMPP as a green powder. Yield: 93.5 wt%. (Found: C, 67.85; H, 4.71; N, 6.26%. Calc. For $C_{50}H_{36}N_4O_5Co \cdot 3H_2O$: C, 67.79; H, 4.78; N, 6.32%). ESI-MS [$CHCl_3$, m/z]: 831 ([CoAPTMPP]$^+$). ^{1}H NMR ($CDCl_3$, 500 MHz): δ 8.85 (*m*, 8H, pyrrole ring), 8.18–8.22 (*d*, $J = 8.5$ Hz, 2H), 8.08–8.10 (*d*, $J = 8.6$ Hz, 6H), 7.51–7.52 (*d*, $J = 8.5$ Hz, 2H), 7.22–7.24 (*d*, $J = 8.6$ Hz, 6H), 6.72–6.78 (*m*, 1H), 6.45–6.51 (*m*, 1H), 6.10–6.12 (*m*, 1H), 4.03 (*s*, 9H).

CoAPTPP, yield: 94.2 wt%. (Found: C, 71.05; H, 4.43; N, 7.11%. Calc. For $C_{47}H_{30}N_4O_2Co \cdot 3H_2O$: C, 70.94; H, 4.56; N, 7.04%). ESI-MS [$CHCl_3$, m/z]: 741 ([CoAPTPP]$^+$). ^{1}H NMR($CDCl_3$, 500 MHz): δ 8.82–8.88 (*m*, 8H, pyrrole ring), 8.23–8.26 (*d*, $J = 8.5$ Hz, 2H), 8.20–8.22 (*d*, $J = 8.3$ Hz, 6H), 7.75 (*m*, 6H), 7.71 (*m*, 3H), 7.53–7.54 (*d*, $J = 8.5$ Hz, 2H), 6.75–6.78 (*m*, 1H), 6.42–6.52 (*m*, 1H), 6.11–6.13 (*m*, 1H).

CoAPTCPP, yield: 95.5 wt%. (Found: C, 62.68; H, 3.65; N, 6.28%. Calc. For $C_{47}H_{27}N_4O_2CoCl_3 \cdot 4H_2O$: C,

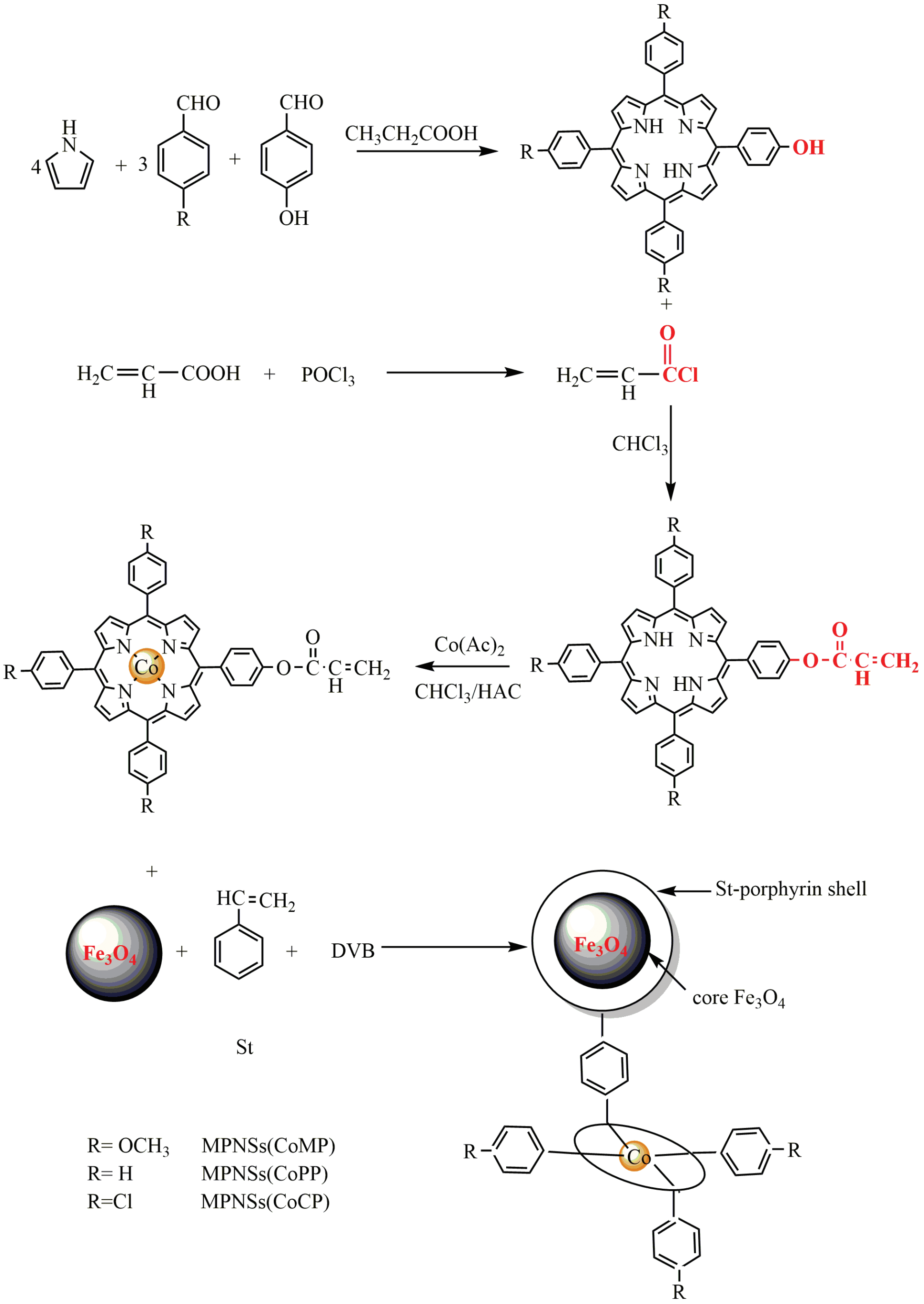

Scheme 1. The strategy to prepare magnetic Co(II) porphyrin nanospheres.

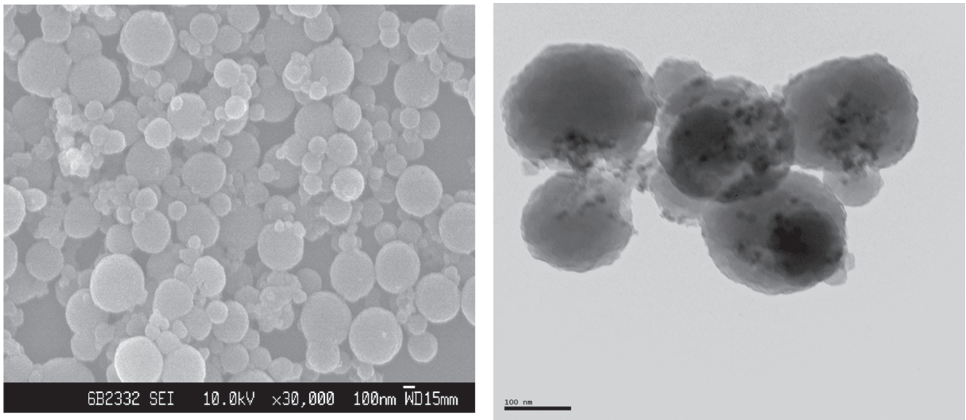

Figure 1. SEM (left) and TEM (right) images of MPNSs(CoMP).

62.79; H, 3.70; N, 6.23%). ESI-MS [$CHCl_3$, m/z]: 845 ([CoAPTCPP]$^+$). ^1H NMR($CDCl_3$, 500 MHz): δ 8.79–8.86 (*m*, 8H, pyrrole ring), 8.16–8.19 (*d*, $J = 8.6$ Hz, 2H), 8.07–8.10 (*d*, $J = 8.5$ Hz, 6H), 7.69–7.71 (*d*, $J = 8.0$ Hz, 6H), 7.52–7.53 (*d*, $J = 8.6$ Hz, 2H), 6.74–6.79 (*m*, 1H), 6.43–6.51 (*m*, 1H), 6.12–6.14 (*m*, 1H).

2.5. Synthesis of MPNSs(CoMP), MPNSs(CoPP) and MPNSs(CoCP)

The strategy to prepare these nanospheres is shown in Scheme 1. A total of 10.0 g magnetic fluid, 12.0 g styrene, 30 mg reactive Co(II) porphyrin acrylate, 3.0 g divinylbenzene (DVB), 1.5 g polyvinylpyrrolidone(K-30) (PVP K-30), 0.30 g 2,2′-azo-bis-isobutyronitrile (AIBN) and 100 mL H_2O/C_2H_5OH were mixed in a 250 mL round-bottomed flask equipped with a reflux condenser. The mixture was stirred at 70 °C for 20–24 h under a N_2 atmosphere. The product was washed with 1 M HCl solution to remove the unenclosed Fe_3O_4 and then with acetone to remove the residual Co(II) porphyrin acrylate. The final product was separated by applying an additional magnetic field (0.42 T) and dried for 24 h at 60 °C in vacuum.

2.6. Catalysis

Cyclohexane hydroxylation catalyzed by metalloporphyrins was carried out in a specially constructed reaction vessel at 30.0 ± 0.1 °C.[10] Using O_2 as the oxidant, the catalytic system consisted of metalloporphyrin or porphyrin nanospheres (the content of porphyrin were 1.29×10^{-3} mmol), coreductant (3.0 mmol ascrobate, 4.0×10^{-2} mmol thiosalicylic acid), substrate (5.55 mmol cyclohexane), acetone/water (9:1, 10 mL) and pure oxygenase (101 kPa). The products were detected after reaction for 3 h by Gas Chromatography using *p*-Chlorotoluene as an internal standard.

The magnetic polymer nanospheres were recovered from the catalytic system by separating in an external magnetic field (0.42 T) after the reaction for 3 h. The hydroxylation of cyclohexane catalyzed by recovered nanospheres was performed under identical conditions.

3. RESULTS AND DISCUSSION

3.1. Characterization of Magnetic Microspheres

The morphology of the magnetic metalloporphyrin nanospheres was obtained by SEM, with satisfying spherical uniformity and average diameter of ca. 300 nm. Meanwhile, the internal structures of these nanospheres were given by TEM, from which one can clearly find the Fe_3O_4 magnetic core embodied in the chitosan shells. Figure 1 gives the SEM and TEM images of MPNSs(CoMP) and Figure 2 shows the size histograms of these nanospheres.

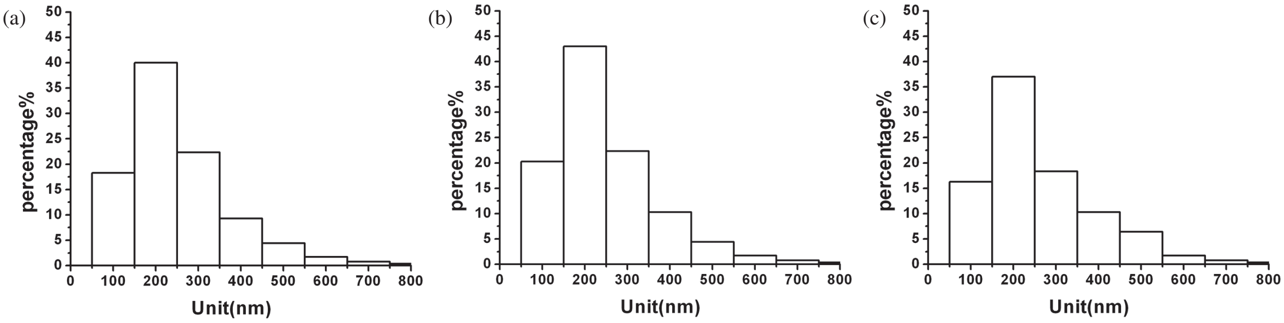

Figure 2. Nanosphere size histograms of MPNSs(CoMP) (a), MPNSs(CoPP) (b) and MPNSs(CoCP) (c).

Negligible difference was found between the nanospheres with different metalloporphyrins.

The presence of metalloporphyrins in the microsphere support was confirmed by solid state UV-Vis spectra as well as ICP results of the catalysts. No substantial UV spectra were observed with the blank magnetic chitosan nanosperes. However, typical absorption spectra of Co(II) porphyrin with Soret bands centered at *ca.* 480 nm and 428 nm, respectively, were observed in the solid state UV-Vis spectra of MPNSs(CoPP) (Fig. 3). Similar results were obtained for the other two nanospheres. The solid state UV-Vis results ambiguously evidenced the existence of metalloporphyrin on the nanospheres. Furthermore, the contents of metalloporphyrins in the magnetic nanospheres were calculated from the contents of Co, which can be obtained using ICP. The contents of metalloporphyrins in microsphere were given in Table I. The ICP results further confirmed the presence of metalloporphyrins in the nanospheres. Meanwhile, the contents of magnetic cores, Fe_3O_4 in the nanospheres were similarly calculated.

IR spectra of these nanospheres are given in Figure 4 and are very similar to each other. Characteristic bands of styrene and Co(II) porphyrin acrylates are shown in the IR spectra of all these nanospheres. For example, the bands in the region of 3100–2900 cm^{-1}, three peaks at 1601, 1491 and 1446. cm^{-1} and double peaks at 758 and 700 cm^{-1} are clearly observed and can be attributed to the benzene rings in styrene. Two peaks at 1024 and 1670 cm^{-1} attributed to the bands of C–O and C=O of Co(II) porphyrin acrylate, respectively, are also observed. All these results suggest that the shell of the nanospheres is composed of copolymer of styrene and Co(II) porphyrin acrylates.

Thermostabilities of the nanospheres have been determined by using thermogravimetric analysis (TGA). The TG curves give us the information that MPNSs(CoMP), MPNSs(CoPP) and MPNSs(CoCP) degrade at 260 °C, 258 °C and 262 °C, respectively. This demonstrates that these catalysts are thermally stable up to almost 260 °C, exhibiting relatively high thermostabilities. The organic parts decompose completely at 483 °C, 446 °C, and 532 °C for MPNSs(CoMP), MPNSs(CoPP) and MPNSs(CoCP), respectively.

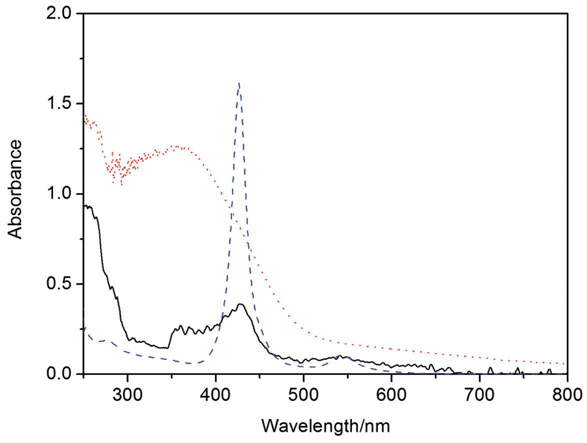

Figure 3. Solid state UV–Vis absorption spectra of MPNSs(CoPP) (solid lines) and blank magnetic nanosperes (red dotted line) as well as CoTPP (blue dash lines).

Table I. Contents of Co(II) porphyrin acrylates and Fe_3O_4 in the nanaospheres.

Catalyst	Co(II) porphyrin acrylate/wt%^{a} (%)	Fe_3O_4/wt% (%)
MPNSs(CoMP)	0.22	6.33
MPNSs(CoPP)	0.16	7.35
MPNSs(CoCP)	0.23	7.69

Note: ^{a}wt% refers to the content of Co(II) porphyrin acrylates in the nanaospheres.

These nanospheres are superparamagnetic and have excellent magnetic responsibility which is the key factor for their effortless recovery. Magnetic hysteresis loops (Fig. 5) show that magnetic nanospheres MPNSs(CoMP) exhibit superparamagnetic behavior with zero coercivity and remanence because the diameter of the magnetic Fe_3O_4 particles used in the preparation of these nanospheres is about 9 nm which is smaller than the critical particle size of Fe_3O_4 particles.[16] Similar results were obtained for the other two nanospheres. The saturation magnetizations of these magnetic nanospheres are almost the same, about 3.50 emu/g, which are lower than that of Fe_3O_4 nanoparticles. It could be explained by the copolymer coating of the Fe_3O_4 nanoparticles in nanospheres.[18]

Furthermore, it was experimentally observed that these nanospheres dispersed in water are rapidly attracted by a conventional magnet placed close to the reaction vessel (Fig. 6), demonstrating the efficacy of magnetic separation.

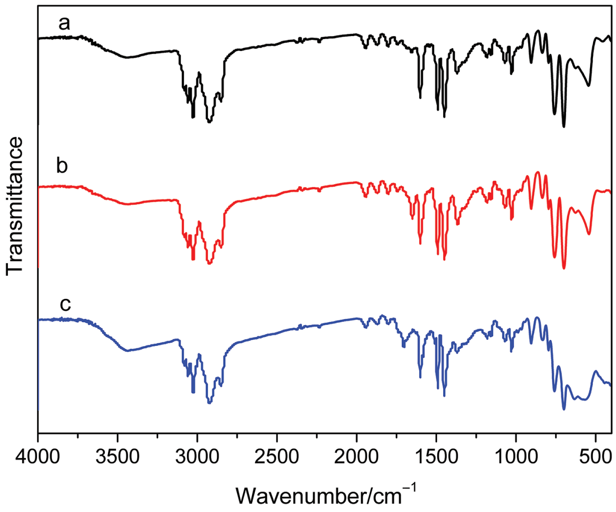

Figure 4. IR spectra of MPNSs(CoMP) (a), MPNSs(CoPP) (b) and MPNSs(CoCP) (c).

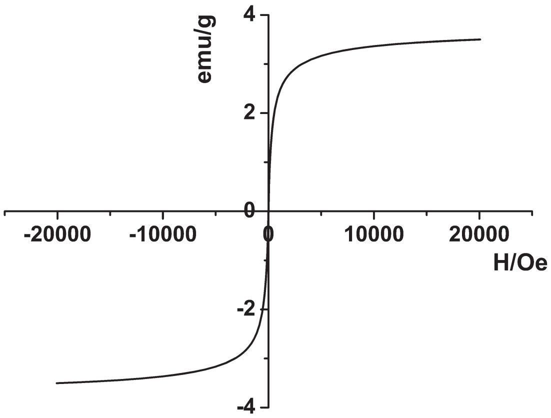

Figure 5. Magnetic hysteresis loops of MPNSs(CoMP).

3.2. Hydroxylation of Cyclohexane Catalysis

3.2.1. The Optimum Catalytic Time

The hydroxylation of cyclohexane catalyzed by these nanospheres was investigated in the Co(II) porphyrin–O_2–ascrobate system. Usually cyclohexanol and cyclohexanone are the main products of the oxidation of cyclohexane in the matelloporphyrin–O_2–ascrobate system under mild conditions.[10] The kinetic curves of turnover numbers for MPNSs(CoMP), MPNSs(CoPP) and MPNSs(CoCP) are shown in Figure 7, from which we can find that the curves have a similar trend, enhancing rapidly and reaching maximum values after about 3 h. The turnover numbers are unchanged with a further increase in the reaction time. These results further suggest that the by-products which come from the over-oxidation of cyclohexanol and cyclohexanone in our reaction system are negligible and 3 h may be the optimum reaction time in the experiments of cyclohexane hydroxylation catalyzed by these catalysts.

3.2.2. The Greatly Enhanced Catalytic Efficiency of Metalloporphyrin Nanospheres

The results of cyclohexane hydroxylation catalyzed by the nanospheres (fresh and recovered) and non-supported Co(II) porphyrin acrylates after reaction for 3 h are listed in Table II. Controlled experiments using styrene-acrylic acid copolymer microspheres or nanopheres with free porphyrins in the presence of $Co(Ac)_2$ as catalysts were carried out and did not lead to substantial product yields (data not shown). From Table II, we can easily find that the three types of nanospheres all have much higher catalytic activities than non-supported Co(II) porphyrin acrylates. The total turnover numbers of the nanospheres are about 200 times larger than those of non-supported Co(II) porphyrin acrylates. As is well known, the hydrophobic microenvironment produced by the protein chain folded around the binding site of cytochrome P450 plays an important role in the process of hydroxylating substrate.[10] However, metalloporphyrins as models of cytochrome P450 have limited catalytic activities to hydroxylate substrate under mild conditions, which may be caused by the lack of this hydrophobic microenvironment. It is believed that the nanospheres provide suitable microenvironment for the "accommodation" of porphyrin catalytic centers[5–10] and thus remarkably enhance the catalytic capability of Co(II) porphyrins.

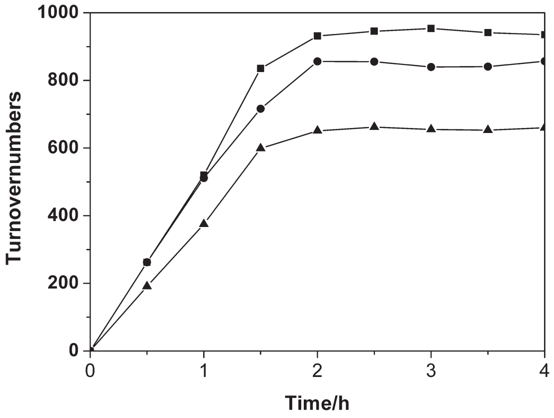

Figure 7. Changes of the turnover numbers of MPNSs(CoMP) (■), MPNSs(CoPP) (●) and MPNSs(CoCP) (▲) calculated from the reaction products with catalytic time.

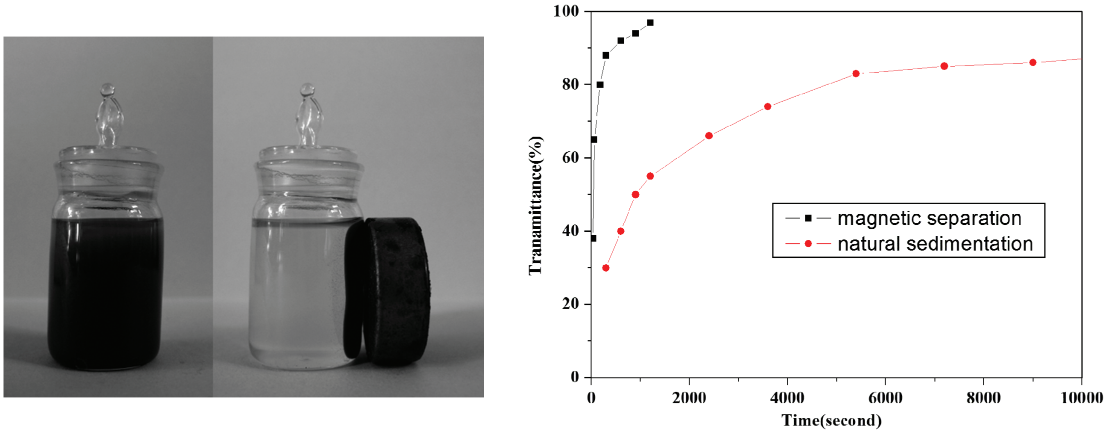

Figure 6. (a): Comparison of the magnetic and natural separation of MCSCoTPP from the liquid media; (b) Transmittance of MCSCoTPP monitored by UV with and without magnetic field.

Table II. The catalytic performance of MPNSs(CoMP), MPNSs(CoPP), MPNSs(CoCP) and Co(II) porphyrin acrylates to hydroxylate cyclohexane after reaction for 3 h.

		Product (turnover number)[c]		
Catalysts[a]	Run[b]	Cyclohexanol	Cyclohexanone	Total
MPNSs(CoMP)	1	51.7 (646)	25.3 (316)	77.0 (962)
	2	50.2 (627)	23.6 (295)	73.8 (922)
	3	51.5 (643)	23.8 (298)	75.3 (941)
	4	52.4 (655)	21.7 (271)	74.1 (926)
	5	51.3 (641)	24.0 (300)	74.3 (941)
MPNSs(CoPP)	1	45.3 (567)	23.5 (294)	68.8 (861)
	2	43.0 (538)	22.1 (276)	65.1 (814)
	3	44.1 (551)	21.2 (265)	65.3 (816)
	4	45.6 (570)	20.7 (259)	66.3 (829)
	5	42.9 (536)	23.1 (289)	66.0 (825)
MPNSs(CoCP)	1	35.8 (448)	17.5 (219)	53.3 (667)
	2	34.5 (431)	16.7 (202)	51.1 (633)
	3	35.1 (439)	17.2 (215)	52.3 (654)
	4	35.2 (440)	16.9 (211)	52.1 (651)
	5	34.6 (432)	17.0 (212)	51.6 (644)
CoAPTMPP	1	3.73 (2.89)	0.94 (0.72)	4.67 (3.61)
CoAPTPP	1	2.98 (2.31)	1.15 (0.89)	4.13 (3.20)
CoAPTCPP	1	2.32 (1.79)	0.77 (0.59)	3.09 (2.38)

Notes: [a]Co(II) porphyrin in the nanospheres and non-supported Co(II) porphyrin acrylates is 0.08 μmol and 1.29 μmol, respectively. [b]The recovery times of catalysis; the non-supported Co(II) porphyrin cannot be recovered. [c]The product (μmol); Turnover number = product(mol)/catalyst(mol).

3.2.3. The Influence of on Porphyrinato Ring Structures

Interestingly, the turnover numbers of the three types of nanospheres under identical conditions follow the order of MPNSs(CoMP) > MPNSs(CoPP) > MPNSs(CoCP) (Table II). It is supposed that the difference in catalytic activity among these magnetic nanospheres is caused by the difference of the phenyl substituents on the porphyrin core. Usually, existence of electron-donating phenyl substituents in the meso-position of porphyrin, such as –OCH_3, will increase the electron density of center metal ions. According to the theory about the catalytic cycle of cytochrome P-450,[6] the increase in electron density of the center metal ion in metalloporphyrin is in favor of reduction of the metal ion, and coordination and activation of dioxygen as well as formation of active intermediate hypervalent metal–oxo species, and thus leads to high catalytic activity of metalloporphyrin. Apparently, the substituent effect also exists in the catalytic process of magnetic nanospheres and the nanospheres with electron-donating p-OCH_3 on porphyrin are more efficient catalysts than those with electron-withdrawing p-Cl groups.

3.2.4. The Recovery and Reuse of Metalloporphyrin Nanospheres

It is notable that these catalysts can be completely recovered and effectively reused although they are nano-sized. As shown in Table II, these catalysts retain their high turnover numbers after being reused five times. There is no loss of magnetic responsiveness or morphological change after recycle. Meanwhile, the UV-Vis and IR spectra of these recovered nanospheres did not show any substantial change compared with those of the fresh ones. The results above provide strong evidence for the stable catalytic capabilities and chemical properties of these catalysts.

Irrespective of their substituents, these magnetic nanospheres immobilizing Co(II) porphyrin are excellent potential candidates for recoverable and reusable catalysts to model P450 enzymes. Moreover, MPNSs(CoMP) exhibit the best catalytic activity among this type of nanospheres.

4. CONCLUSIONS

We have prepared three types of novel magnetic polymer nanospheres immobilizing Co(II) porphyrin appending different phenyl substituents and have investigated their catalysis to hydroxylate cyclohexane. These core/shell structured nanospheres are of an average diameter of *ca.*200 nm and have good magnetic responsiveness. The turnover numbers of these nanospheres to hydroxylate cyclohexane are much larger than those of non-supported Co(II) porphyrin acrylates under identical conditions and follow the order of MPNSs(CoMP) >MPNSs(CoPP) > MPNSs(CoCP).

Electron-donating groups on the periphery of porphyrins can enhance the catalytic activity of the nanospheres. Moreover, these magnetic nanospheres can be effectively recovered and can retain their high catalytic activity after being recycled five times. These results may facilitate the design of high-efficient, environmental-friendly metalloporphyrin catalysts.

Acknowledgments: This work was financially supported by the National Nature Science Foundation of China (21101033).

References and Notes

1. J. T. Groves and W. J. Kruper, *J. Am. Chem. Soc.* 101, 7613 **(1979)**.
2. S. Ritter, *Chem. Eng. News Archive* 90, 7 **(2012)**.
3. K. Mittra, S. Chatterjee, S. Samanta, and A. Dey, *Inorg. Chem.* 52, 14317 **(2013)**.
4. C. Q. Ma, D. Xing, C. W. Zhai, J. W. Che, S. Y. Liu, J. Wang, and W. H. Hu, *Org. Lett.* 15, 6140 **(2013)**.
5. C. Monnereau, P. H. Ramos, A. B. C. Deutman, J. A. A. W. Elemans, R. J. M. Nolte, and A. E. Rowan, *J. Am. Chem. Soc.* 132, 1529 **(2010)**.
6. G. Huang, L. Q. Mo, J. L. Cai, X. Cao, Y. Peng, Y. A. Guo, and S. J. Wei, *Appl. Catal. B* 162, 364 **(2015)**.
7. J. Li, J. P. Lei, Q. B. Wang, P. Wang, and H. X. Ju, *Electrochim. Acta* 83, 73 **(2012)**.
8. F. Zadehahmadi, S. Tangestaninejad, M. Moghadam, V. Mirkhani, I. M. Baltork, A. R. Khosropour, and R. Kardanpour, *J. Solid State Chem.* 218, 56 **(2014)**.
9. S. L. H. Rebelo, M. Linhares, M. M. Q. Simões, A. M. S. Silva, M. G. P. M. S. Neves, J. A. S. Cavaleiro, and C. Freire, *J. Catal.* 315, 33 **(2014)**.

10. J. W. Huang, W. J. Mei, J. Liu, and L. N. Ji, *J. Mol. Catal. A* 170, 261 (**2001**).

11. S. M. G. Pires, M. M. Q. Simões, C. M. S. Santos, S. L. H. Rebelo, F. A. A. Paz, M. Graça P. M. S. Neves, and J. A. S. Cavaleiro, *Appl. Catal. B* 160–161, 80 (**2014**).

12. A. Modak, J. Mondal, and A. Bhaumik, *Appl. Catal. A* 459, 41 (**2013**).

13. C. Eichholz, J. Knoll, D. Lerche, and H. Nirschl, *J. Magn. Magn. Mater.* 368, 139 (**2014**).

14. J. Han, Y. Zhuo, Y. Q. Chai, Y. Q. Yu, N. Liao, and R. Yuan, *Anal. Chim. Acta* 790, 24 (**2013**).

15. S. Ghasemi, M. Heidary, M. Faramarzi, and Z. Habibi, *J. Mole. Catal.* 100, 121 (**2014**).

16. Y. X. Wang, H. Q. Sun, H. M. Ang, M. O. Tadé, and S. B. Wang, *J. Colloid Interface Sci.* 433, 68 (**2014**).

17. F. X. Chen, R. Liu, S. W. Xiao, and C. T. Zhang, *Mater. Res. Bull.* 55, 38 (**2014**).

18. J. M. Hong and Y. He, *Desalination* 332, 67 (**2014**).

19. A. C. S. Sekhar, K. Sivaranjani, C. S. Gopinath, and C. P. Vinod, *Catal. Today* 198, 92 (**2012**).

20. K. Nishioka, S. Horita, K. Ohdaira, and H. Matsumura, *Sol. Energy Mater. Sol. Cells* 92, 919 (**2008**).

21. K. Nishioka, T. Sueto, and N. Saito, *Appl. Surface Sci.* 255, 9504 (**2009**).

22. W. Y. Xie, D. J. West, Y. Y. Sun, and S. B. I. Zhang, *Nano. Energy* 2, 742 (**2013**).

23. K. Rad-Moghadam and N. Dehghan, *J. Mol. Catal. A* 392, 97 (**2014**).

24. S. Zakavi, A. G. Mojarrad, and S. Rayati, *J. Mol. Catal. A* 363–364, 153 (**2012**).

Received: 11 December 2014. Accepted: 21 November 2015.